J Mol Model (2013) 19:2473–2483
DOI 10.1007/s00894-013-1777-0

ORIGINAL PAPER

A temperature–concentration (T–X) phase diagram calculated using the mean field theory for liquid crystals

Hamit Yurtseven · Selami Salihoglu · Huseyin Karacali

Received: 10 October 2012 / Accepted: 18 January 2013 / Published online: 24 February 2013

Abstract Phase-line equations for smectic–hexatic phase transitions in liquid crystals were derived using the Landau phenomenological theory. In particular, second-order transitions for the smectic-A–smectic-C (SmA–SmC) and hexatic-B–hexatic-F (or HexI) transitions were studied and the tricritical points for these transitions were located. The calculated phase-line equations were fitted (using experimental data for various liquid crystals) to construct a generalized *T–X* phase diagram. It was shown that the *T–X* phase diagram calculated from the free energy adequately describes the observed behavior of liquid crystals during smectic–hexatic transitions.

Keywords Mean field theory · Phase diagram · Liquid crystals

Introduction

Transitions among isotropic liquid, nematic, and smectic phases have been the subject of a number of studies, as reported in the literature. The transitions that occur between isotropic liquid and nematic (IN), between nematic and smectic-A (NA), between smectic-A and smectic-C or C* (AC or AC*), and also between smectic-C (or C*) and crystal (solid) phases as the temperature is decreased have been investigated both experimentally and theoretically in many liquid-crystalline systems. Thermodynamic and some dynamic quantities have been measured or calculated at various temperatures, pressures, and concentrations for these transitions in liquid crystals. Phase diagrams (*T–P* or *X–T*) have also been constructed based on the experimental measurements and theoretical models.

Transitions from smectic phases (untilted SmA and tilted SmC) to hexatic phases (untilted HexB and tilted HexF or HexI) have also been investigated for various liquid-crystalline materials. It has been reported [1–8] that some liquid crystals freeze into plastic crystals (CrE or CrB) at low temperatures close to their HexB–HexF (or HexI) transition.

Transitions among the various smectic and hexatic phases can be classified as either first or second order, resulting in the existence of triple points and tricritical points (TCPs). Phase lines among the phases SmA, HexB, and HexF (or HexI), which are first-order lines, meet at a triple point. Phase lines among the phases SmA, SmC, and Hex F (or Hex I) also give rise to a triple point for these first-order smectic–hexatic transitions. Although most smectic–hexatic transitions are first order, there are also second-order phase lines between untilted (SmA) and tilted (SmC) smectic phases and between untilted (HexB) and tilted (HexF or HexI) hexatic phases. The point at which first-order and second-order lines intersect for both SmA–SmC and HexB–HexF (HexI) transitions is known as the tricritical point (TCP), as shown in a generalized phase diagram [8] (Fig. 1). The phase diagram for binary mixtures of 650BC and 40.8 has also been obtained [3, 4]. This exhibits untilted phases: SmA, HexB, CrB, and CrE.

This phase diagram includes smectic (SmA and SmC) phases which become hexatic (untilted HexB and tilted HexF and HexI) phases. The vertical axis is $(T - T_{BOO})$, where T_{BOO} is the smectic–hexatic transition temperature. For

H. Yurtseven (✉)
Department of Physics, Middle East Technical University, 06531 Ankara, Turkey
e-mail: hamit@metu.edu.tr

S. Salihoglu
Department of Physics, Istanbul Technical University, Maslak, Istanbul, Turkey
e-mail: salihogl@itu.edu.tr

H. Karacali
Department of Physics, Abant Izzet Baysal University, 14280 Gölköy Bolu, Turkey
e-mail: karacali_h@ibu.edu.tr

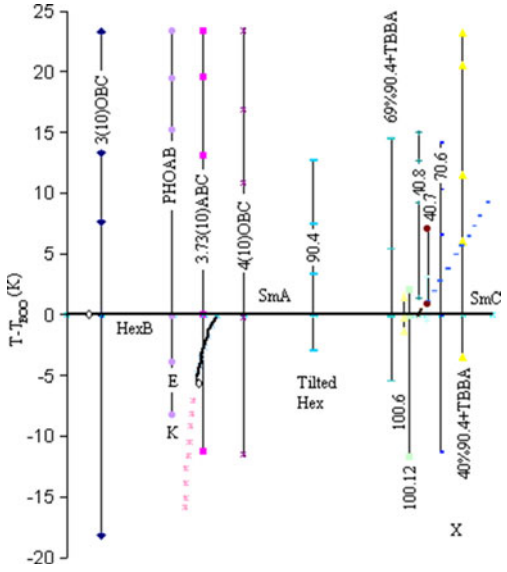

Fig. 1 Generalized smectic–hexatic phase diagram [8]. Equations 3.2 and 3.6 were fitted to the *solid* (first-order) and *dotted* (second-order) *lines*; the values of the fitted parameters are shown in Tables 1 and 2. The *light vertical lines* represent temperature ranges over which the SmA and hexatic phases are stable. All the tilted hexatic phases shown are HexF except for those of 3.73(10) OBC and 4(10) OBC [8]. Tricritical points (TCP's) are denoted by small circles between the solid and dotted lines fort he SmA-SmC and HexB-HexF (Hex I)transitions

fixed concentrations of various liquid crystals, the unoriented axis is the composition variable X [8] with varying temperatures along the T-T_{BOO} axis, as shown in Fig. 1. For a homologous series such as n(10) OBC, the composition X can take integer or noninteger values. When n is nonintegral, as in 3.73(10) OBC (Fig. 1), the nonintegral value denotes a binary mixture of two adjacent homologs (73 wt % 4(10) OBC). Below the x-axis, all vertical lines represent transitions from untilted (HexB) and tilted (HexF and I) to plastic crystal phases (CrB, CrG, and the rigid crystal K). The dotted lines in Fig. 1 are used for second-order transition lines and solid lines indicate first-order transition lines. TCPs are positioned along the curve between HexB and tilted HexF (or HexI) and along the curve between SmA and SmC.

It has been proposed [8] that the SmA–HexB transition can be considered weakly first order, with some smeared, minor latent heat effects rounding the the C_p peaks. Given that the effective heat capacity (C_p) exponent of α_{eff} ranges between 0.5 and 0.65 [9, 10], and that between 0.15 and 0.25 [11, 12], it was concluded that SmA-HexB transitions exhibit 3D-XY critical behaviour. [8]. Among the hexatic phases that exhibit long-range bond orientational order (BOO) but short-range plane positional order, it has been suggested [5, 8] that the HexB phase is a fluctuation-induced phase that is sensitive to positional order. For tilted phases (SmC and HexF or HexI), the tilt angle θ can couple with the bond orientational order parameter ψ, and the tilt can modify the bond orientational order parameter (BOO) in Sm C and Hex F (or Hex I) phases. This coupling between θ and ψ has been studied in some theoretical models [13], as have herringbone order [14], positional density [15, 16], and smectic layer fluctuations [17]. For plastic crystal phases near HexB–HexF (or HexI) transitions, it has been suggested that there is short-range HexF (or HexI) order in the HexB phase and that there is short-range HexB order in the HexF (or HexI) phase [8].

Within the framework of the mean field model introduced in this study, the following points motivated us to investigate smectic–hexatic phase transitions in binary mixtures of liquid crystals:

(i) Phase coexistence can be described in a mixture of liquid crystals that occurs in a finite temperature range at a fixed concentration in the smectic–hexatic transition model.

(ii) The concentration dependence of the latent heat can be obtain in a similar way we have obtained the concentration dependence of the Gibbs free energy for the smectic-hexatic transition here

(iii) Features of the TCP that occurs for the smectic–hexatic transition and also the mean field to tricritical crossover behavior can be characterized by the quadrupole–quadrupole interactions (by the coupling term $\psi^2\theta^2$ in the free-energy expansion).

(iv) The critical behavior of the susceptibility χ and the specific heat C_P between the smectic and hexatic phases and near the TCP can be described in binary mixtures of liquid crystals. This is achieved by minimizing the free energy with respect to the order parameters (the bond orientational order parameter ψ and tilt angle θ). Thus, the temperature and concentration dependences of both χ and C_P can be obtained by minimization, and the temperature and concentration dependences of ψ and θ can also be obtained. Therefore, the critical behavior of the order parameters (ψ and θ), the susceptibility χ, and the specific heat C_P can be considered to be temperature and concentration dependent.

(v) Similarly, the temperature and concentration dependences of other thermodynamic quantities such as the thermal expansivity α_p and the isothermal compressibility κ_T can be derived using the mean field model, and the critical behavior of each near the smectic–hexatic transitions for mixtures of liquid crystals can be described.

(vi) By choosing the concentration dependence of the coupling constant (c of $\psi^2\theta^2$ in the free-energy expansion) appropriately, the order of the transition (first order, second order, or tricritical) between smectic and hexatic phases can be characterized for mixtures of liquid crystals. As an example, in the case of mixtures of ferroelectric liquid crystals, X=0 corresponds to a pure

ferroelectric material which exhibits a first-order transition, $X=1$ is the concentration of a nonferroelectric material which exhibits a second-order transition, and $0<X<1$ corresponds to a transition between first order and second order or tricritical (for a fixed X value), as we have shown previously [18].

(vii) By determining the concentration dependence of the temperature shift, $\Delta T=T_C - T_0$, where T_0 is the transition temperature and T_C is the experimental temperature, the order of the transition (first order, second order, or tricritical) can be characterized, as we have shown previously [18]. For a second-order transition, $\Delta T=0$.

(viii) The coupling of the order parameters with the concentration is an important determinant of the phase behavior and the order of the transition.

(ix) The correlation between the orientational order parameter and the enthalpy (linear or nonlinear) can be established for hexatic–smectic transitions in binary mixtures of liquid crystals.

In the study described in the present paper, we expanded the free energy for smectic–hexatic transitions in terms of the bond orientational order (BOO) parameter ψ and the tilt angle θ. By minimizing the free energy with respect to the order parameters (ψ and θ), we derived the phase-line equations for SmA–HexB, SmA–HexF, SmA–SmC, HexB–HexF, and SmC–HexF transitions. These phase-line equations were fitted to experimental data [8] for various liquid crystals that exhibit smectic–hexatic transitions. In this treatment, quadratic coupling between the order parameters ψ and θ was considered in the free-energy expansion, just as we did for SmA–SmC* transitions in previous studies [18–20]. The coefficient of the quadratic term ψ^2 was assumed to depend on the temperature and the concentration for various binary mixtures of liquid crystals, as observed experimentally, and all other coefficients in the free-energy expansion were taken to be constant. Thus, a generalized T-X diagram was constructed for smectic–hexatic transitions by fitting the phase-line equations to experimental data [8]. We have calculated the phase diagrams for the liquid crystals near the nematic-SmA-SmC (NAC) [21, 22] and the nematic-SmA-SmC* (NAC*) [23] points previously. Very recently, we derived [24] phase-line equations for first-order SmA–HexF, SmA–HexB, SmA–SmC, HexB–HexF, and SmC–HexF transitions in liquid crystals and calculated a generalized smectic–hexatic phase diagram using experimental data [8]. In the present study, we derived the phase-line equations for the first-order transitions stated above and for second-order SmA–SmC and HexB–HexF transitions by calculating the T–X phase diagram using mean field theory. However, aside from the SmA–HexB transition, the first-order SmA–HexF, SmA–SmC, HexB–HexF, and SmC–HexF transitions were treated differently in the work reported in the present paper compared to the approach used in our previous work [24], although we used the same experimental data [8] in the present study as was used in our previous study [24]. Additionally, in the present work, we calculated the Gibbs free energy as a function of concentration for smectic–hexatic transitions of a few liquid crystals used as examples.

In the next section, we derive the phase-line equations according to the Landau phenomenological theory. In the section after that, we provide our calculations and results. We then discuss those results and draw conclusions based on them in subsequent sections.

Theory

The free energy can be expanded in terms of the order parameters according to the Landau phenomonological theory. By taking the temperature and pressure (or concentration) dependences of the coefficients in the free-energy expansion, thermodynamic quantities can be predicted near phase transitions. Using these dependences of the coefficients, the phase-line equations can be derived for the transitions studied. By predicting the first-order and second-order phase lines, temperature–pressure (T–P) or the temperature–concentration (T–X) phase diagrams can be constructed.

In this study, we construct a generalized T–X phase diagram for smectic liquid crystals that form hexatic phases upon cooling, using the Landau phenomenological theory. The first-order and second-order phase-line equations for the relevant smectic–hexatic transitions are derived from the free-energy expansion. In particular, for SmA–SmC and HexB–HexF transitions, the TCP at which the first-order and second-order phase lines intersect is located. The phase-line equations derived here are fitted to the experimental T–P phase diagram for the smectic–hexatic transitions of various liquid crystals [8]. The values of the fitted parameters and the coordinates of the TCPs for the transitions studied are determined. The relationship between the Gibbs free energy of mixing and the concentration—which is used to construct the T–X phase diagram via the Landau phenomenological theory—is also demonstrated here, using the SmA–HexB transitions for liquid crystals of 3(10) OBC and PHOAB (Fig. 1) as examples (see Fig. 2).

Below, we derive the phase-line equations of various smectic–hexatic transitions.

SmA–HexB transition

The free energy of the SmA phase is

$$F_A = 0. \tag{2.1}$$

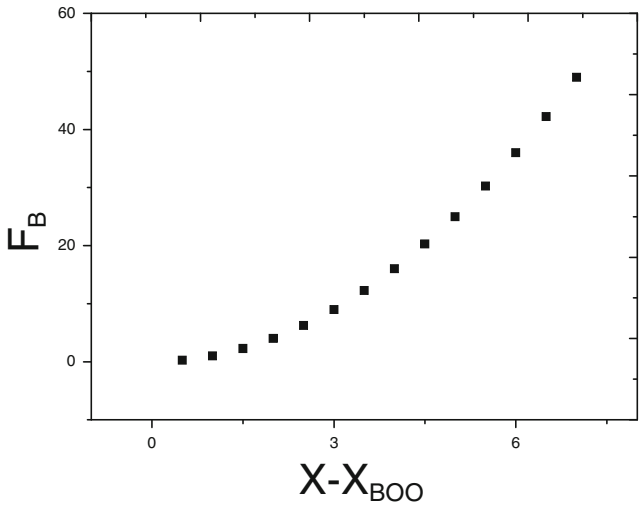

Fig. 2 Gibbs free energy of the hexatic-B (HexB) phase as a function of the concentration X (calculated according to Eq. 3.8) for the SmA–HexB transitions of the liquid crystals mentioned in Fig. 1

The free energy of the HexB phase can be expressed in terms of the order parameter ψ as

$$F_B = a_2\psi^2 + a_4\psi^4 + a_6\psi^6, \tag{2.2}$$

where $a_2 > 0$, $a_4 < 0$ and $a_6 > 0$ for the first-order SmA–HexB transition. The first-order condition gives

$$F_A = F_B, \tag{2.3}$$

so that

$$a_2\psi^2 + a_4\psi^4 + a_6\psi^6 = 0. \tag{2.4}$$

By minimizing the free energy F_B with respect to the order parameter ψ, we get

$$a_2 + 2a_4\psi^2 + 3a_6\psi^4 = 0. \tag{2.5}$$

From Eqs. 2.4 and 2.5, we have

$$\psi^2 = -\frac{a_4}{2a_6}. \tag{2.6}$$

By inserting Eq. 2.6 into Eq. 2.4, we then get

$$\frac{a_4}{8a_6^2}\left(a_4^2 - 4a_2a_6\right) = 0 \tag{2.7}$$

or

$$a_4^2 = 4a_2a_6. \tag{2.8}$$

This is the phase-line equation for the SmA–HexB transition.

SmA–HexF transition

The free energy of the HexF phase is

$$F_F = a_2\psi^2 + a_4\psi^4 + a_6\psi^6 + b_2\theta^2 + b_4\theta^4 + b_6\theta^6 + c\psi^2\theta^2, \tag{2.9}$$

where $a_2 > 0$, $a_4 < 0$, $a_6 > 0$, $b_2 > 0$, $b_4 < 0$, and $b_6 > 0$.

The first-order condition is

$$F_A = F_F. \tag{2.10}$$

This gives

$$a_2\psi^2 + a_4\psi^4 + a_6\psi^6 + b_2\theta^2 + b_4\theta^4 + b_6\theta^6 + c\psi^2\theta^2 = 0. \tag{2.11}$$

By minimizing F_F with respect to ψ, we obtain

$$a_2 + 2a_4\psi^2 + 3a_6\psi^4 + c\theta^2 = 0. \tag{2.12}$$

Also, by minimizing F_F with respect to θ, we obtain

$$b_2 + 2b_4\theta^2 + 3b_6\theta^4 + c\psi^2 = 0. \tag{2.13}$$

From Eq. 2.12, we have a solution for θ:

$$\theta^2 = -\frac{1}{c}\left(a_2 + 2a_4\psi^2 + 3a_6\psi^4\right). \tag{2.14}$$

From Eq. 2.13, we have also a solution for ψ:

$$\psi^2 = -\frac{1}{c}\left(b_2 + 2b_4\theta^2 + 3b_6\theta^4\right). \tag{2.15}$$

By substituting Eq. 2.14 into Eq. 2.15, we then get

$$A_1\psi^8 + A_2\psi^6 + A_3\psi^4 + A_4\psi^2 + A_5 = 0, \tag{2.16}$$

where

$$\begin{aligned} A_1 &= -27a_6^2b_6/c^3 \\ A_2 &= -36a_4a_6b_6/c^3 \\ A_3 &= 6\left(a_6b_4c - 2a_4^2b_6 - 3a_2a_6b_6\right)/c^3 \\ A_4 &= \left(4a_4b_4c - 12a_2a_4b_6 - c^3\right)/c^3 \\ A_5 &= \left(2a_2b_4c - 3a_2^2b_6 - b_2c^2\right)/c^3 \end{aligned} \tag{2.17}$$

Let us rewrite Eq. 2.16 in terms of the B coefficients:

$$B_1\psi^8 + B_2\psi^6 + B_3\psi^4 + B_4\psi^2 + B_5 = 0. \tag{2.18}$$

By choosing B_1=1, the B coefficients can be related to the A coefficients as follows:

$$\begin{aligned} B_2 &= \tfrac{A_2}{A_1} = \tfrac{4a_4}{3a_6} \\ B_3 &= \tfrac{A_3}{A_1} = \tfrac{2}{9a_6^2b_6}\left(2a_4^2b_6 + 3a_2a_6b_6 - a_6b_4c\right) \\ B_4 &= \tfrac{1}{27a_6^2b_6}\left(12a_2a_4b_6 - 4a_4b_4c + c^3\right) \\ B_5 &= \tfrac{1}{27a_6^2b_6}\left(3a_2^2b_6 + b_2c^2 - 2a_2b_4c\right) \end{aligned} \tag{2.19}$$

We can also rewrite Eq. 2.16 in terms of the C coefficients:

$$C_1\psi^8 + C_2\psi^6 + C_3\psi^4 + C_4\psi^2 + C_5 = 0. \quad (2.20)$$

By taking C_1=a_6, the other C coefficients can be related to the B coefficients as follows:

$$\begin{aligned} C_2 &= a_6B_2 = \tfrac{4a_4}{3} \\ C_3 &= a_6B_3 = \tfrac{2}{9a_6b_6}\left(2a_4^2b_6 + 3a_2a_6b_6 - a_6b_4c\right) \\ C_4 &= a_6B_4 = \tfrac{1}{27a_6b_6}\left(12a_2a_4b_6 - 4a_4b_4c + c^3\right) \\ C_5 &= a_6B_5 = \tfrac{1}{27a_6b_6}\left(3a_2^2b_6 + b_2c^2 - 2a_2b_4c\right) \end{aligned} \quad (2.21)$$

Let us choose C_5=0. This gives

$$3a_2^2b_6 + b_2c^2 - 2a_2b_4c = 0. \quad (2.22)$$

By inserting C_5=0 into Eq. 2.20, we obtain the free energy expanded up to ψ^6 as

$$C_1\psi^6 + C_2\psi^4 + C_3\psi^2 + C_4 = 0. \quad (2.23)$$

Let us also choose C_4=0. From Eq. 2.21, we have

$$12a_2a_4b_6 - 4a_4b_4c + c^3 = 0. \quad (2.24)$$

Using Eq. 2.22, we then get the coupling constant as

$$c = \left[a_2b_4 \pm \left(a_2^2b_4^2 - 3a_2^2b_2b_6\right)^{1/2}\right]/b_2. \quad (2.25)$$

By assuming that the discriminant $\Delta = 0$ in Eq. 2.25, we find that

$$b_4^2 = 3b_2b_6. \quad (2.26)$$

The coupling constant then becomes

$$c = a_2b_4/b_2. \quad (2.27)$$

Inserting Eq. 2.27 into Eq. 2.24 gives

$$a_2^2b_4^3 + 12a_4b_2^3b_6 - 4a_4b_2^2b_4^2 = 0. \quad (2.28)$$

Since it is not a simple task to satisfy Eqs. 2.25 or 2.27 and 2.28 simultaneously, we can make both C_4 and C_5 zero by choosing a_6 to be a very large number (see Eq. 2.21). Hence,

$$a_6 \gg 1. \quad (2.29)$$

In that case, Eq. 2.20 becomes

$$C_1\psi^4 + C_2\psi^2 + C_3 = 0. \quad (2.30)$$

This equation can be solved for ψ^2 as

$$\psi^2 = \frac{-C_2 \pm \sqrt{C_2^2 - 4C_1C_3}}{2C_1}. \quad (2.31)$$

Since a_4 is negative,

$$-\frac{C_2}{C_1} = \frac{2|a_4|}{3a_6} \rangle 0. \quad (2.32)$$

In Eq. 2.31, the discriminant becomes

$$\Delta = C_2^2 - 4C_1C_3 = \frac{8a_6}{9b_6}\left(|b_4|c - 3a_2b_6\right), \quad (2.33)$$

meaning that

$$\frac{\Delta^{1/2}}{2C_1} = \frac{1}{2a_6^{1/2}}\left[\frac{8}{9b_6}\left(|b_4|c - 3a_2b_6\right)\right]^{1/2}. \quad (2.34)$$

When Eqs. 2.32 and 2.34 are substituted into Eq. 2.31 by taking the positive solution, we get

$$\psi^2 = \frac{2}{3}\frac{|a_4|}{a_6} + \frac{1}{2a_6^{1/2}}\left[\frac{8}{9b_6}\left(|b_4|c - 3a_2b_6\right)\right]^{1/2}. \quad (2.35)$$

Since a_6 is very large, we can ignore the first term in Eq. 2.35. Hence,

$$\psi \cong \frac{1}{\sqrt{2}a_6^{1/4}}\left[\frac{8}{9b_6}\left(|b_4|c - 3a_2b_6\right)\right]^{1/4}. \quad (2.36)$$

Equation 2.36 can be rewritten as

$$\psi = \frac{1}{\sqrt{2}}\left(\frac{8}{9}\frac{|b_4|c}{a_6b_6} - \frac{8a_2}{3a_6}\right)^{1/4}. \quad (2.37)$$

If we ignore the second term in Eq. 2.37 because a_6 is very large, we have

$$\psi = \left(\frac{2}{9}\frac{|b_4|c}{a_6b_6}\right)^{1/4}, \quad (2.38)$$

where the coupling constant c is positive. In order to get the maximum value of ψ ($\cong 1$), we choose the ratio in Eq. 2.38 to be

$$|b_4|c/a_6b_6 \cong 9/2 \quad (2.39)$$

By inserting Eq. 2.38 back into Eq. 2.14, we then obtain

$$\theta^2 = -\frac{a_2}{c} - \frac{2}{3}\frac{|b_4|}{b_6} + \frac{2|a_4|}{c}\left(\frac{2}{9}\frac{|b_4|c}{a_6b_6}\right)^{1/2}. \quad (2.40)$$

Consequently, by choosing a_2 to be finite, $c > 0$, and a_6 and a_4 to be large, we can express the order parameters ψ and θ as shown in Eqs. 2.38 and 2.40, respectively. Nothing that a_2 is small, and choosing b_6 to be large, just as we did for a_6 , we can ignore the first two terms in Eq. 2.40. θ^2 can therefore be written as

$$\theta^2 = \frac{2|a_4|}{c}\left(\frac{2}{9}\frac{|b_4|c}{a_6b_6}\right)^{1/2}. \quad (2.41)$$

Using these expressions for ψ (Eq. 2.38) and θ^2 (Eq. 2.41) in Eq. 2.11, we then obtain the phase-line

equation for the SmA–HexF transition. After some algebra, we find that

$$\frac{2}{3}\frac{|a_4||b_4|c}{a_6b_6}-\frac{8}{9}\frac{|a_4|^2|b_4|^2}{ca_6b_6}+\left(a_2+\frac{2b_2|a_4|}{c}\right)\left(\frac{2}{9}\frac{|b_4|c}{a_6b_6}\right)^{1/2}+\left(a_6+\frac{8b_6|a_4|^3}{c^3}\right)\left(\frac{2}{9}\frac{|b_4|c}{a_6b_6}\right)^{3/2}=0. \tag{2.42}$$

SmA–SmC transition

The free energy of the SmA phase is zero, as before. The free energy of the SmC phase can be expressed as

$$F_C=c_2\psi^2+c_4\psi^4+c_6\psi^6+d_2\theta^2+d_4\theta^4+d_6\theta^6+c\psi^2\theta^2, \tag{2.43}$$

where ψ is very small. In Eq. 2.43, $c_2>0$, $c_4<0$, $c_6>0$, $d_2>0$, $d_4<0$, and $d_6>0$.

Minimizing F_C with respect to ψ gives

$$c_2+2c_4\psi^2+3c_6\psi^4+c\theta^2=0. \tag{2.44}$$

Also, minimizing F_C with respect to θ gives

$$d_2+2d_4\theta^2+3d_6\theta^4+c\psi^2=0. \tag{2.45}$$

By taking a_6 to be a large number, Eqs. 2.44 and 2.45 yield

$$\psi=\frac{1}{\sqrt{2}}\left(\frac{8}{9}\frac{|d_4|c}{a_6d_6}-\frac{8c_2}{3c_6}\right)^{1/4}, \tag{2.46}$$

as given by Eq. 2.37 for the SmA–HexF transition. By taking $|d_4|$, d_6 to be finite, c_2 to be small, and c_6 to be very large, we can ignore the second term in Eq. 2.46. We then get

$$\psi=\left(\frac{2}{9}\frac{|d_4|c}{c_6d_6}\right)^{1/4}, \tag{2.47}$$

where c is positive, similar to Eq. 2.38. Inserting this value of ψ into F_C (Eq. 2.43) gives

$$F_C=c_2\left(\tfrac{2}{9}\tfrac{|d_4|c}{c_6d_6}\right)^{1/2}+c_4\left(\tfrac{2}{9}\tfrac{|d_4|c}{c_6d_6}\right)+c_6\left(\tfrac{2}{9}\tfrac{|d_4|c}{c_6d_6}\right)^{3/2}+d_2\theta^2+d_4\theta^4+d_6\theta^6+c\theta^2\left(\tfrac{2}{9}\tfrac{|d_4|c}{c_6d_6}\right)^{1/2}. \tag{2.48}$$

For the second-order part of the SmA–SmC transition, the coefficient of θ^2 should be zero. Hence, from Eq. 2.48, we have

$$d_2+c\left(\frac{2}{9}\frac{|d_4|c}{c_6d_6}\right)^{1/2}=0. \tag{2.49}$$

This is the phase-line equation for the second-order part of the transition between the SmA and SmC phases. At the tricritical point (TCP), we should have

$$d_4=0. \tag{2.50}$$

For the first-order part of the SmA–SmC transition, we insert the value of ψ given by Eq. 2.47 into Eq. 2.44. We then get

$$\theta^2=-\frac{c_2}{c}-\frac{2}{3}\frac{|d_4|}{d_6}+\frac{2|c_4|}{c}\left(\frac{2}{9}\frac{|d_4|c}{c_6d_6}\right)^{1/2}, \tag{2.51}$$

similar to Eq. 2.40 for the SmA–HexF transition. By choosing

$$|d_4|c/c_6d_6\cong 9/2, \tag{2.52}$$

in Eq. 2.47 (as given in Eq. 2.39), we obtain the maximum value of $\psi(\cong 1)$, similar to Eq. 2.41 for the SmA–HexF transition. Thus, the order parameters ψ and θ are expressed by Eqs. 2.47 and 2.51, respectively, where c_2 is finite (positive), $c>0$, and c_6 and c_4 are large. Since c_2 is small, and by choosing d_6 large as a_6, the first two terms in Eq. 2.51 can be ignored. The θ^2 expression can then be written as

$$\theta^2=\frac{2|c_4|}{c}\left(\frac{2}{9}\frac{|d_4|c}{c_6d_6}\right)^{1/2}. \tag{2.53}$$

If we use the expressions for ψ (Eq. 2.47) and θ^2 (Eq. 2.53) in Eq. 2.43 with

$$F_A=F_C=0, \tag{2.54}$$

which gives

$$c_2\psi^2+c_4\psi^4+c_6\psi^6+d_2\theta^2+d_4\theta^4+d_6\theta^6+c\psi^2\theta^2=0, \tag{2.55}$$

we can derive the phase-line equation for this transition. We find that

$$\frac{2}{3}\frac{|c_4||d_4|c}{c_6d_6}-\frac{8}{9}\frac{|c_4|^2|d_4|^2}{cc_6d_6}+\left(c_2+\frac{2d_2|c_4|}{c}\right)\left(\frac{2}{9}\frac{|d_4|c}{c_6d_6}\right)^{1/2}+\left(c_6+\frac{8d_6|c_4|^3}{c^3}\right)\left(\frac{2}{9}\frac{|d_4|c}{c_6d_6}\right)^{3/2}=0. \tag{2.56}$$

This is the first-order part of the SmA–SmC transition.

HexB–HexF transition

We first obtain the second-order phase line between the HexB and HexF phases. The free energy F_B of the HexB phase is given by Eq. 2.2. Also, the free energy F_F of the HexF phase is given by Eq. 2.9. By minimizing the free

energy F_F with respect to the order parameters ψ and θ, we get Eqs. 2.12 and 2.13, respectively. Using the same treatment given for the SmA–HexF transition, we end up with an expression for the order parameter ψ (Eq. 2.38) for the HexB–HexF transition. By inserting Eq. 2.38 into the free energy F_F expression (Eq. 2.9), we find

$$F_F = a_2\left(\frac{2}{9}\frac{|b_4|c}{a_6 b_6}\right)^{1/2} + a_4\left(\frac{2}{9}\frac{|b_4|c}{a_6 b_6}\right) + a_6\left(\frac{2}{9}\frac{|b_4|c}{a_6 b_6}\right)^{3/2} + b_2\theta^2 + b_4\theta^4 + b_6\theta^6 + c\theta^2\left(\frac{2}{9}\frac{|b_4|c}{a_6 b_6}\right)^{1/2}, \quad (2.57)$$

similar to Eq. 2.48 for the SmA–SmC transition. For the second-order phase line of the HexB–HexF transition, the coefficient of θ^2 in Eq. 2.57 should be equal to zero. Hence, we have

$$b_2 + c\left(\frac{2}{9}\frac{|b_4|c}{a_6 b_6}\right)^{1/2} = 0, \quad (2.58)$$

which is essentially the same relation (Eq. 2.49) as given for the SmA–SmC transition. At the TCP, we should have

$$b_4 = 0. \quad (2.59)$$

Now we can derive the first-order phase line between the HexB and HexF phases, as we did for the SmA–SmC transition. θ^2 can be obtained from Eq. 2.12 for the HexF phase, as shown by Eq. 2.14. Similarly, ψ^2 can be obtained from Eq. 2.13 (see Eq. 2.15). Using the first-order condition that

$$F_B = F_F = 0, \quad (2.60)$$

which gives

$$b_2 + b_4\theta^2 + d_6\theta^4 + c\psi^2 = 0, \quad (2.61)$$

it is possible to determine the phase-line equation for the HexB–HexF transition. By minimizing the free energy F_B of the HexB phase (Eq. 2.2) with respect to ψ, we get Eq. 2.5, which can be solved for ψ^2. This gives

$$x = \psi^2 = \frac{-a_4 + \left(a_4^2 - 3a_2a_6\right)^{1/2}}{3a_6}. \quad (2.62)$$

When we substitute Eq. 2.62 into Eq. 2.61, we get

$$b_2 + b_4\theta^2 + b_6\theta^4 + cx = 0. \quad (2.63)$$

Since a_2 is small and a_6 is large, we can ignore the second term in Eq. 2.62, which gives

$$\psi^2 = \frac{-a_4}{3a_6}. \quad (2.64)$$

Equation 2.63 then becomes

$$b_6\theta^4 + b_4\theta^2 + \left(b_2 - \frac{a_4c}{3a_6}\right) = 0, \quad (2.65)$$

which can be solved for θ^2 as

$$\theta^2 = -\frac{b_4}{2b_6} + \frac{\left[b_4^2 - 4\left(b_2 - \frac{a_4c}{3a_6}\right)b_6\right]^{1/2}}{2b_6}. \quad (2.66)$$

By choosing b_2 to be small, b_6 to be large, and a_4 and b_6 to be finite, the second term in Eq. 2.66 can also be ignored, meaning that θ^2 becomes

$$\theta^2 = \frac{-b_4}{2b_6}. \quad (2.67)$$

Finally, by substituting the expressions for ψ^2 (Eq. 2.64) and θ^2 (Eq. 2.67) into Eq. 2.63, we find that

$$12b_2a_6b_6 - 6b_4a_6 + 3b_4^2a_6 - 4a_4b_6c = 0. \quad (2.68)$$

This is the first-order phase line for the HexB–HexF transition.

SmC–HexF transition

The free energies of the HexF and SmC phases are given by Eqs. 2.9 and 2.43, respectively, by assuming the same coupling constant c. In the SmC phase, ψ is very small, whereas it is large in the HexF phase.

When we minimize F_F (Eq. 2.9) with respect to the order parameters ψ and θ, we get Eqs. 2.12 and 2.13, respectively, as before. Using the expressions for θ^2 (Eq. 2.14) and ψ^2 (Eq. 2.15) for the HexF phase, and following the same procedure as given for the SmA–HexF transition, we obtain ψ for the HexF phase (Eq. 2.38). Similarly, using the same procedure as employed for the SmA–SmC transition, we can find ψ for the SmC phase (Eq. 2.47). When we substitute Eq. 2.38 into Eq. 2.14, we obtain an expression for θ^2 (given by Eq. 2.40), which can be reduced to Eq. 2.41 for the HexF phase. Similarly, for the SmC phase, our final expression for θ^2 is given by Eq. 2.53. We then insert Eqs. 2.38 and 2.41 into F_F (Eq. 2.9) and Eqs. 2.47 and 2.53 into F_C (Eq. 2.43). Using the first-order condition that

$$F_F = F_C, \quad (2.69)$$

we finally obtain the phase-line equation between the SmC and HexF phases. After some algebra, F_F is obtained as

$$F_F = \left(a_2 + \frac{2|a_4|b_2}{c}\right)\left(\frac{2}{9}\frac{|b_4|c}{a_6 b_6}\right)^{1/2} + |a_4| \times \left(1 + \frac{4|a_4|b_4}{c^2}\right)\left(\frac{2}{9}\frac{|b_4|c}{a_6 b_6}\right) + \left(a_6 + \frac{8|a_4|^3 b_6}{c^3}\right)\left(\frac{2}{9}\frac{|b_4|c}{a_6 b_6}\right)^{3/2}. \quad (2.70)$$

Similarly, F_C can be obtained as

$$F_C = \left(c_2 + \frac{2|c_4|d_2}{c}\right)\left(\frac{2}{9}\frac{|d_4|c}{c_6 d_6}\right)^{1/2} + |c_4| \times \left(1 + \frac{4|c_4|d_4}{c^2}\right)\left(\frac{2}{9}\frac{|d_4|c}{c_6 d_6}\right) + \left(c_6 + \frac{8|c_4|^3 d_6}{c^3}\right)\left(\frac{2}{9}\frac{|d_4|c}{c_6 d_6}\right)^{3/2}. \quad (2.71)$$

Using Eq. 2.69, the first-order phase-line equation for the HexF–SmC transition is given by

$$\left(a_2 + \frac{2|a_4|b_2}{c}\right)\left(\frac{2}{9}\frac{|b_4|c}{a_6 b_6}\right)^{1/2} + |a_4|\left(1 + \frac{4|a_4|b_4}{c^2}\right)\left(\frac{2}{9}\frac{|b_4|c}{a_6 b_6}\right) + \left(a_6 + \frac{8|a_4|^3 b_6}{c^3}\right)\left(\frac{2}{9}\frac{|b_4|c}{a_6 b_6}\right)^{3/2} = \left(c_2 + \frac{2|c_4|d_2}{c}\right)\left(\frac{2}{9}\frac{|d_4|c}{c_6 d_6}\right)^{1/2} + |c_4|\left(1 + \frac{4|c_4|d_4}{c^2}\right)\left(\frac{2}{9}\frac{|d_4|c}{c_6 d_6}\right) + \left(c_6 + \frac{8|c_4|^3 d_6}{c^3}\right)\left(\frac{2}{9}\frac{|d_4|c}{c_6 d_6}\right)^{3/2}. \quad (2.72)$$

Calculations and results

The phase-line equations that we derived as shown above were used to calculate a generalized smectic–hexatic (T–X) phase diagram for various liquid crystals that were measured experimentally [8]. By assuming that the temperature and concentration dependences of the coefficients exhibited the functional forms given in the phase-line equations for the transitions studied here, it was possible to fit the phase-line equations to the observed data and thus determine the fitted parameters. The coordinates of the tricritical points (TCPs) were also determined for the SmA–SmC and HexB–HexF transitions, which exhibit both first-order and second-order features. The SmA–HexB, SmA–HexF, and SmC–HexF transitions are only first order.

SmA–HexB transition

The phase-line equation for the SmA–HexB transition is given by Eq. 2.8. By assuming that the coefficient a_2 depends on the temperature and concentration as

$$a_2 = a_{20}(T - T_{BOO}) + a_{21}(X - X_{BOO})^2, \quad (3.1)$$

and that a_4 and a_6 are constant, the phase line described by Eq. 2.8 can be written as follows:

$$T - T_{BOO} = \alpha_0 + \alpha_1 X + \alpha_2 X^2. \quad (3.2)$$

In Eq. 3.1, a_{20} and a_{21} are constant. In Eq. 3.2, the coefficients α_0, α_1, and α_2 are constant. T_{BOO} represents the transition temperature for the bond orientational order (BOO) parameter ψ. Equation 3.2 was fitted to the experimental data for the SmA–HexB transition [8]. Since the SmA–HexB transition line occurs at $T-T_{BOO}=0$ [8], as shown in Fig. 1, the coefficients are all equal to zero ($\alpha_0=\alpha_1=\alpha_2=0$).

SmA–HexF transition

In the phase-line equation given by Eq. 2.42 for the SmA–HexF transition, we assumed that the temperature and concentration dependence of coefficient a_2 is given by Eq. 3.1, whereas that of coefficient b_2 can be written as

$$b_2 = b_{20}(T - T_{BOO}) + b_{21}(X - X_{BOO})^2. \quad (3.3)$$

By choosing the coefficients a_4, b_4, a_6, b_6, and c in Eq. 2.42 to be constant, it was possible to fit the phase-line equation (Eq. 2.42) to the experimental $T-T_{BOO}$ vs. X phase diagram [8] shown in Fig. 1. Just as for the SmA–HexB transition, the SmA–HexF transition occurs at $T-T_{BOO}=0$, which leads to the coefficients $\alpha_0=\alpha_1=\alpha_2=0$.

SmA–SmC transition

Since the SmA–SmC transition involves first- and second-order phase lines, which meet at the TCP, both phase-line equations were considered in this work. First, the phase-line equation of the second-order part (Eq. 2.49) was fitted to the experimental data (Fig. 1) according to Eq. 3.2 with coefficients α_0, α_1, and α_2. We assumed that the coefficients depend on temperature and concentration as

$$d_2 = d_{20}(T - T_{BOO}) + d_{21}(X - X_{BOO})^2, \quad (3.4)$$

where d_{20} and d_{21} are constants. Upon fitting Eq. 2.49 to the observed data along the transition line between the SmA and SmC phases [8], the coefficients α_0, α_1, and α_2 were determined (during this fitting process, d_4, d_6, and c were taken to be constant in Eq. 2.49). The values of the fitted parameters α_0, α_1, and α_2 for the second-order part of the SmC transition are given in Table 1. The temperature and concentration coordinates for the TCP are also indicated in Table 1.

For the first-order line of the SmA–SmC transition, the phase-line equation (Eq. 2.56) was fitted to Eq. 3.2, just as we did for the second-order part of this transition. In Eq. 2.56, we assumed that

$$c_2 = c_{20}(T - T_{BOO}) + c_{21}(X - X_{BOO})^2, \quad (3.5)$$

and that the temperature and concentration dependence of the coefficient d_2 is given by Eq. 3.4. In both equations, c_{20}, c_{21}, d_{20}, and d_{21} are constant. When Eq. 2.56 was fitted to Eq. 3.2, the coefficients α_0, α_1, and α_2 were determined,

Table 1 Values of the parameters obtained upon fitting Eq. 3.3 to the experimental data [8] for the phase transition indicated. The coordinates of the tricritical point (TCP) are also given. T_{BOO} is the smectic–hexatic transition temperature

SmA–SmC	α_0 (K)	α_1 (K/wt %)	α_2 (K/wt %)^2	$T - T_{BOO}$ (K)	X (wt %)
First order	31.82	−7.30	0.33	0.86	16.74
Second order	−46.26	2.82	0	0.86	16.74

and these values are shown in Table 1. In this table, we also give the values of the temperature and concentration at the TCP for the first-order part of the SmA–SmC transition. Those values are the same as those for the second-order part of this transition (Table 1).

HexB–HexF transition

Just like the SmA–SmC transition, the HexB–HexF transition is both first and second order. Both phase lines coincide at the TCP. For the second-order line described by Eq. 2.58, the temperature and concentration dependence of the coefficient b_2 was assumed here to be the same as Eq. 3.5, whereas the coefficients b_4, a_6, b_6, and c were taken to be constant. Thus, by expressing Eq. 2.58 in the same form as Eq. 3.2, we obtained

$$T - T_{BOO} = \beta_0 + \beta_1 X + \beta_2 X^2. \tag{3.6}$$

Under the assumption given above, Eq. 3.6 was fitted to the observed data for the second-order part of the HexB–HexF transition (Fig. 1). The values of the fitted parameters β_0, β_1, and β_2 are given in Table 2. We also provide the coordinates of the TCP for the second-order part of the HexB–HexF transition in this table.

Regarding the first-order part of the HexB–HexF transition, we wrote the phase-line equation (Eq. 2.68) in the same functional form as Eq. 3.6, based on the assumption that the coefficient b_2 depends on the temperature and concentration as described by Eq. 3.3, and that the coefficients b_4, a_6, b_6, and c are all constant. By fitting Eq. 3.6 to the observed data for the first-order part of the HexB–HexF transition (Fig. 1), the values of the fitted parameters β_0, β_1, and β_2 were determined, as tabulated in Table 2. We also give the coordinates of the TCP for the first-order part of the HexB–HexF transition in this table.

SmC–HexF transition

The first-order SmC–HexF transition is described by the phase-line equation (2.72). As we did for the previous transitions, we assumed the following temperature and concentration dependences (shown in parentheses) of the coefficients: a_2 (Eq. 3.1), b_2 (Eq. 3.3), c_2 (Eq. 3.5), and d_2 (Eq. 3.4) in Eq. 2.72. We also assumed that the coefficients a_4, a_6, b_4, b_6, c_4, c_6, d_4, and d_6, as well as the coupling constant c, were constant. Under this assumption, the phase-line equation for the SmC–HexF transition (Eq. 2.72) was rewritten in the form of Eq. 3.6. When Eq. 3.6 was fitted to the experimental phase line at $T-T_{BOO}=0$, the fitted parameters were obtained as $\beta_0=\beta_1=\beta_2=0$, similar to the SmA–HexB and SmA–HexF transitions (Fig. 1).

Gibbs free energy as a function of concentration

The T–X phase diagram can be deduced from the relationship between the Gibbs free energy of mixing and the concentration, as stated above. In the Landau phenomenological theory, the Gibbs free energy can be expanded in terms of the order parameters. By minimizing the Gibbs free energy with respect to the order parameters and assuming the temperature and concentration dependences of the coefficients given in the free-energy expression, the T–X phase diagram can be constructed. As an example, in the case of smectic-A–hexatic-B (SmA–HexB) phase transitions in liquid crystals (Fig. 1), the variation of the Gibbs free energy with the concentration can be obtained within the framework of the mean field theory. Using the Gibbs free energy of the hexatic-B (HexB) phase (Eq. 2.2) along with the following concentration dependence of the coefficient a_2 (Eq. 3.1):

$$a_2 = a_{21}(X - X_{BOO})^2, \tag{3.7}$$

Table 2 Parameter values obtained by fitting Eq. 3.6 to the experimental data [8] for the phase transition indicated. The coordinates of the TCP are also given. T_{BOO} is the smectic–hexatic transition temperature

HexB–HexF	β_0 (K)	β_1 (K/wt %)	β_2 (K/wt %)^2	$T - T_{BOO}$ (K)	X (wt %)
First order	−206.74	56.87	−3.91	−6.05	6.06
Second order	−1085.5	353.78	−28.99	−6.25	6.06

the relationship between the Gibbs free energy (F_B) and the concentration X was obtained. In Eq. 3.1, $T - T_{BOO}=0$ (Eq. 3.2) because of the SmA–HexB transition line for the liquid crystals of 3(10) OBC, PHOAB, 3.73(10)OBC, and 4(10) OBC (Fig. 1), as also pointed out in the section "SmA–HexB transition." Thus, the Gibbs free energy (Eq. 2.2) can be written as follows using Eq. 3.7:

$$F_B = A(X - X_{BOO})^2, \tag{3.8}$$

where A is another constant given by

$$A = -\frac{a_{21}a_4}{2a_6}\left(1 + \frac{a_4^2}{4a_6}\right), \tag{3.9}$$

since we assume that a_4 and a_6 are constants. Equation 3.8 gives the quadratic dependence of the Gibbs free energy (F_B) on the concentration (X), as plotted in Fig. 2 for the SmA–HexB transitions of the liquid crystals given above (Fig. 1). Similarly, the Gibbs free energy as a function of concentration can be obtained for the SmA–HexF transition (see the section "SmA–HexF transition"), the SmA–SmC transition (see "SmA–SmC transition"), the HexB–HexF transition (see "HexB–HexF transition"), and the SmC–HexF transition (see "SmC–HexF transition"). Thus, the concentration dependences of the Gibbs free energy for both HexF (F_F by Eq. 2.9) and SmC (F_C by Eq. 2.43) can be obtained. F_F and F_C can then be plotted as a function of X for liquid crystals that exhibit the phase transitions shown in Fig. 1.

Discussion

In this work, phase-line equations were derived by expanding the free energy in terms of the order parameters (the bond orientational order parameter ψ and the tilt angle θ) using the Landau phenomenological theory. Quadratic coupling between ψ and θ in the free-energy expansion was considered. When quadratic coupling ($\theta^2\psi^2$) was applied, the bond orientational order (BOO) paremeter ψ was taken to be very small in SmC phase, whereas in the hexatic-F (or Hex I) phase this parameter was large for the smectic-hexatic transitions studied here. The phase-line equations were fitted to the experimental phase lines for various liquid crystals exhibiting smectic–hexatic phase transitions, as shown in Fig. 1. As stated above, among the smectic–hexatic transitions studied here, SmA–SmC and HexB–HexF (tilted hexatic) transitions contain both first-order and second-order features, with phase lines that meet at the tricritical point (TCP), which we determined in this work (Tables 1 and 2). Regardless of whether the first-order or the second-order phase line was used to calculate the TCP for the SmA–SmC transition, the TCP was located at the same temperature and concentration coordinates (Table 1). The temperature coordinate of the TCP for the HexB–HexF transition differed by about 0.20 K depending on whether it was calculated using the first-order or second-order phase line (Table 2).

In the fitting procedure, the phase-line equations for the SmA–HexB (Eq. 2.8), SmA–HexF (Eq. 2.42), and SmA–SmC (Eqs. 2.49 and 2.56) transitions were reduced to Eq. 3.2 by assuming the temperature and concentration dependences of the coefficients a_2 (Eq. 3.1), b_2 (Eq. 3.3), c_2 (Eq. 3.5), and d_2 (Eq. 3.4). We also reduced the phase-line equations for the HexB–HexF (Eqs. 2.58 and 2.68), and SmC–HexF (Eq. 2.72) transitions to Eq. 3.6 by assuming the temperature and concentration dependences of the coeffiicents a_2 (Eq. 3.1), b_2 (Eq. 3.3), c_2 (Eq. 3.5), and d_2 (Eq. 3.4). These assumptions were made because it was difficult to fit the phase-line equations in their derived form to the experimental data due to the large number of parameters in these equations. By reducing the number of parameters in the phase-line equations to just three (Eqs. 3.2 and 3.6), we were able to calculate the T-X phase diagram foe liquid crystals that exhibit smectic-hexatic phase transitions to the data in the experimental phase diagram (Fig. 1).

Since we derived the functional forms of the order parameters ψ and θ from the free-energy expansion for smectic–hexatic transitions in various liquid crystals, it was then possible to predict their temperature and concentration dependences, as stated above. In particular, for the SmA–HexB transition, the ψ^2 expansion (Eq. 2.6) indicated that the bond orientational order parameter is constant on the phase line, since a_4 and a_6 were taken to be constant. This was not the case for the SmA–HexF (tilted hexatic phase) transition (see Eqs. 2.14 and 2.15 for the tilt angle θ and the bond orientational order parameter ψ, respectively). For this transition, both order parameters were found to depend on the temperature and concentration because of the assumed functional forms of a_2 (Eq. 3.1) and b_2 (Eq. 3.3). This was also seen for the SmA–SmC transition, as both ψ (Eq. 2.46) and θ (Eq. 2.51) were obtained as functions of c_2, which depends on the temperature and concentration (see Eq. 3.5). Note that these order parameters were assumed to be constant in the simplified forms of ψ (Eq. 2.47) and θ (Eq. 2.53) for the SmA–SmC transition. Similarly, the order parameters ψ (Eq. 2.62) and θ (Eq. 2.66) for the HexB–HexF transition were found to be dependent on the temperature and concentration due to the coefficients a_2 (Eq. 3.1) and b_2 (Eq. 3.3). Again, they were taken to be constant on the phase line of the HexB–HexF transition in their reduced forms (Eqs. 2.64 and 2.67). Finally, for the SmC–Hex F transition, the order parameters ψ (Eq. 2.15) and θ (Eq. 2.14) were shown to be temperature and concentration dependent because of the functional forms of the coefficients a_2 (Eq. 3.1) and b_2 (Eq. 3.3).

We also investigated the relationship between the Gibbs free energy of mixing and the concentration using the SmA–HexB transition as an example. In this case, a quadratic relationship was obtained (see Eq. 3.8; Fig. 2). This is the simplest form of the Gibbs free energy according to Eq. 2.2, obtained when a_4 and a_6 were taken to be constants and $T - T_{BOO}=0$ for 3(10) OBC and PHOAB (Fig. 1). On the other hand, when $T - T_{BOO}\neq 0$ and the coefficient a_4 depends on both temperature and concentration (a_6 is constant), the Gibbs free energy depends on the concentration in a more complicated form, such that a number of parameters need to be adjusted to the experimental data. This dependence is even more complicated for the other transitions (the SmA–HexF, SmA–SmC, HexB–HexF, and SmC–HexF transitions), since the functional forms of the Gibbs free energy for those phases are not as simple as Eq. 2.2.

Finally, using the Landau phenomenological theory, we developed a mean field model that describes the general features of the bond orientational order parameter, tilt angle, dielectric susceptibility, and other thermodynamic quantities for the hexatic–smectic transitions of various binary mixtures of liquid crystals using a *T–X* phase diagram. The temperature and concentration dependences of those thermodynamic quantities can be predicted by our mean field model. By choosing appropriate Landau coefficients in the free energy, it is possible to construct the *T–X* or *T–P* phase diagrams. The phase diagram as well as thermodynamic, light-scattering, and X-ray experiments are required to accurately characterize the order of transitions between hexatic and smectic phases in binary mixtures of liquid crystals.

Conclusions

A generalized *T–X* phase diagram was constructed in this study using the Landau phenomenological theory. In this approach, the free energy was expanded in terms of the order parameters ψ (bond orientational order parameter) and θ (tilt angle) for smectic–hexatic transitions. The phase-line equations derived were fitted to experimental *T–X* data and the values of the fitted parameters were determined. We focused in particular on the second-order phase lines, and the tricritical points (TCPs) were located for SmA–SmC and HexB–HexF (or HexI) transitions.

The temperature and concentration dependences of the order parameters ψ and θ were predicted from the free-energy expansion. The concentration dependence of the Gibbs free energy was also derived for the SmA–HexB transition. The temperature and concentration dependences of some other thermodynamic quantities, such as the specific heat, thermal expansion, and isothermal compressibility, can be gauged from the free-energy expansion given here for smectic–hexatic transitions in liquid crystals. Our predictions for the order parameters ψ and θ, as well as the thermodynamic quantities that can be derived, can be compared with experimental measurements of various liquid crystals that exhibit smectic–hexatic transitions.

References

1. Lushington KJ, Kasting GB, Garland CW (1980) J Phys (Paris) Lett 41:L419
2. Bloemen E, Garland CW (1981) J Phys (Paris) 42:1299
3. Goodby JW, Pindak R (1981) Mol Cryst Liq Cryst 75:233
4. Huang CC (1983) Phys Rev A28:2433
5. Mahmood R, Lewis M, Johnson D, Surrendranath V (1988) Phys Rev A 38:4299
6. Huang CC, Nounesis G, Geer R, Goodby JW, Guillon D (1989) Phys Rev A 39:3741
7. Iannacchione G, Gorecka E, Pyzuk W, Kumar S, Finotello D (1995) Phys Rev E 51:3346
8. Kutnjak Z, Garland CW (1998) Phys Rev E 57:3015
9. Huang CC, Stoebe T (1993) Adv Phys 42:343
10. Haga H, Kutnjak Z, Iannacchione G, Qian S, Finotello D, Garland CW (1997) Phys Rev E 56:1808
11. Gorecka E, Chen L, Kumar S, Krowczynski A, Pyzuk W (1994) Phys Rev E 50:2863
12. Gorecka E, Chen L, Lavrentovich A, Pyzuk W (1994) Europhys Lett 27:507
13. Defontaines AD, Prost J (1993) Phys Rev E 47:1184
14. Bruinsma R, Aeppli G (1982) Phys Rev Lett 48:1625
15. Aeppli G, Bruinsma R (1984) Phys Rev Lett 53:2133
16. Aharony A, Birgeneau RJ, Brock JD, Litster LD (1986) Phys Rev Lett 57:1012
17. Selinger JV (1988) J Phys (Paris) 49:1387
18. Yurtseven H, Kurt M (2011) Int J Mod Phys B 425:1791
19. Salihoğlu S, Yurtseven H, Giz A, Kayışoğlu D, Konu A (1998) Phase Trans 66:259
20. Salihoğlu S, Yurtseven H, Bumin B (1998) Int J Mod Phys B 12:2083
21. Tüblek A, Yurtseven H, Salihoğlu S (1998) Phase Trans 64:203
22. Yurtseven H, Enginer Y, Salihoğlu S (2000) Calphad 24:483
23. Salihoğlu S, Tüblek A, Yurtseven H (2000) Phase Trans 70:263
24. Yurtseven H, Karacali H (2012) Phys Chem Liq 50:302